15th World Congress on Computational Mechanics (WCCM-XV)
8th Asian Pacific Congress on Computational Mechanics (APCOM-VIII)
Virtual Congress: 31 July – 5 August 2022
S. Koshizuka (Ed.)

SIMULATION OF STRETCHING DEFORMATION OF FILM FOR ELECTRONIC DEVICES IN ATUOMOTIVE APPLICATIONS

JIHONG LIU[1], AKIO HIGAKI[1], NOBUYUKI KOMATSU[1] AND SATORU TAKANEZAWA[1]

[1]Daikin Industries, Ltd.
1-1 Nishi-Hitotsuya, Settsu, Osaka 566-8585, Japan
jihong.liu@daikin.co.jp, https://www.daikin.com/

Key words: Finite Element Method, Orthogonal Anisotropic Plasticity, Transverse Stretching, Fluorine Film, Thickness, Kink Band

Abstract. *In this study, we proposed a simulation method for film transverse stretching based on the finite element method using the orthogonal anisotropy plastic model. The simulation method can analyse the large deformation of film stretching and predict whether the kink band phenomenon occurs during the film transverse stretching. The validity of the simulation method was confirmed by the transverse stretching tests performed on the fluorine films with different longitudinal stretching ratios. Using the simulation method, we clarified that the plastic anisotropy index of the longitudinally stretched fluorine film has a great influence on the presence or absence of the kink band phenomenon during the film transverse stretching. The plastic anisotropy index of the longitudinally stretched fluorine film can be related to its birefringence, and the two are approximately in a linear relationship. Moreover, we revealed the change in film stretching deformation due to difference in the ratio of the stretching zone length to the width of the tenter.*

1 INTRODUCTION

Fluoropolymers have excellent weather resistance, heat resistance and electrical insulation properties, and are used in a wide range of fields such as semiconductors and automobiles [1]. Recently, it has been clarified that the electrical properties such as relative permittivity, volume resistivity and dielectric breakdown strength of the fluoropolymers can be significantly improved by controlling their crystal structure with biaxial stretching [2]. As a result, biaxially stretched fluorine films are increasingly expected to be used in automobile-related electronic devices such as high-frequency substrate films, motor insulating papers, and film capacitors to improve their performances and reduce their sizes and weights. For example, the sizes and weight of the film capacitors can be reduced to less than half with the fluorine films compared to polypropylene (PP) films. As automobiles become CASE (Connected, Autonomous, Shared, Electric) vehicles, various devices are required to be smaller and lighter. The downsizing of the film capacitors will greatly contribute to the miniaturization and performance improvement of the electronic devices for electric vehicles. However, since the fluoropolymers have a lower rigidity than other polymers such as polyethylene terephthalate (PET) and PP, it is difficult to continuously manufacture the fluorine films because kink bands and stretching tears are easily to occur during the transverse stretching of successive biaxial stretching with a tenter.

Several studies have been conducted on deformation behavior during stretching of films such as PET. Yamada et al. [3-5] performed experimental and analytical studies on the bowing deformation of the film during the transverse stretching. They observed the bowing deformation profile throughout a tenter in a pilot plant of successive biaxial stretching and clarified the effect of the temperature of the thermosetting zone and the cooling zone on the bowing deformation. At the same time, they also compared the experimental results with simulation ones obtained with finite element method to elucidate the mechanism of bowing deformation and proposed a way to decrease bowing deformation of film by inserting a cooling zone between the transverse stretching zone and thermosetting zone. The bowing deformation means that a straight line drawn across the width of the longitudinally stretched film is deformed into a bow shape after transverse stretching by a tenter. It usually causes the anisotropy of film characteristics such as the heat shrinkage and mechanical properties. Sugihara et al. [6] predicted the influences of temperature on the bowing phenomenon of amorphous cyclo-olefin-polymer (COP) film in a tenter of successive biaxial stretching process with finite element method based on elasto-plastic theory. Tokihisa et al. [7] studied the deformation behavior of PP film under different draw ratios along machine direction to optimize stretching conditions on transverse stretching. However, for fluoropolymers having lower rigidity than PET and PP, kink band phenomenon which causes film rupture is observed in addition to the bowing deformation during transverse stretching. No studies have been found on the simulation of the kink band phenomenon that easily occurs in stretching of low-rigidity polymers such as fluoropolymers until now.

In this study, we proposed a simulation method for film transverse stretching based on the finite element method using the orthogonal anisotropy plastic model. The simulation method can not only analyse the large stretching deformation up to the orientation hardening region, but also predict the kink band phenomenon that occurs during the film transverse stretching. The validity of the simulation method was confirmed by the transverse stretching tests performed on the fluorine film with different longitudinal stretching ratios. Using the simulation method, we clarified that the plastic anisotropy index of the fluorine film has a great influence on the presence or absence of the kink band phenomenon during the film transverse stretching. The plastic anisotropy index of the fluorine film after longitudinal stretching can be related to its birefringence, and the two are approximately in a linear relationship. Moreover, we revealed the change in film stretching deformation due to difference in the ratio of the stretching zone length to the width of the tenter.

2 FILM STRETCHING METHOD

The successive biaxial stretching method with a tenter is widely used for the industrial production of film such as PP, PET and COP due to its high productivity. Figure 1 shows the schematic diagram of the film stretching method [8], which mainly consist of the longitudinal machine direction (MD) stretching and the transverse direction (TD) stretching. MD represents the traveling direction of the film, and TD represents the width direction of the film. As shown in Fig.1, the extruder melts, and extrudes the polymer. The extruded polymer is cast on a chill roll to form an amorphous sheet. The sheet is subsequently stretched in the longitudinal direction by the rollers with different rotational speeds to form a uniaxial oriented film. The uniaxial-oriented film which is held by the tenter clips is then stretched in the transverse direction to form the biaxial oriented film.

In this study, a pilot plant with a tenter schematically shown in Fig.1 is used for experimental production of the biaxial oriented fluorine film. The transverse stretching is usually performed using a tenter. As schematically depicted in Fig.2, the tenter usually consists of four zones: preheating, stretching, thermosetting, and cooling. Here, L_1, L_2, L_3 and L_4 in the figure are the lengths of each zone, α is the inclination angle of the stretching zone, and W_0 and W_1 are the widths of the film after longitudinal stretching and transverse stretching, respectively. The length of each zone of the tenter used in this study is described in Table 1.

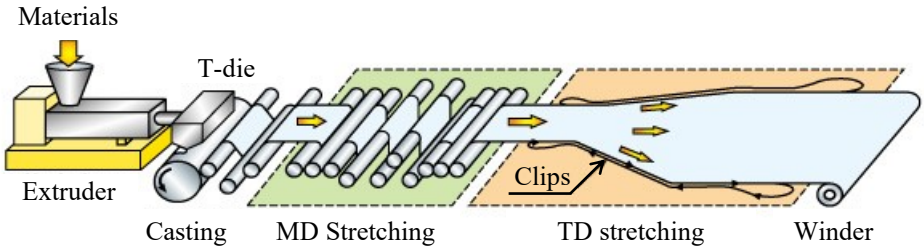

Figure 1: Schematic diagram of film successive biaxial stretching process with a tenter

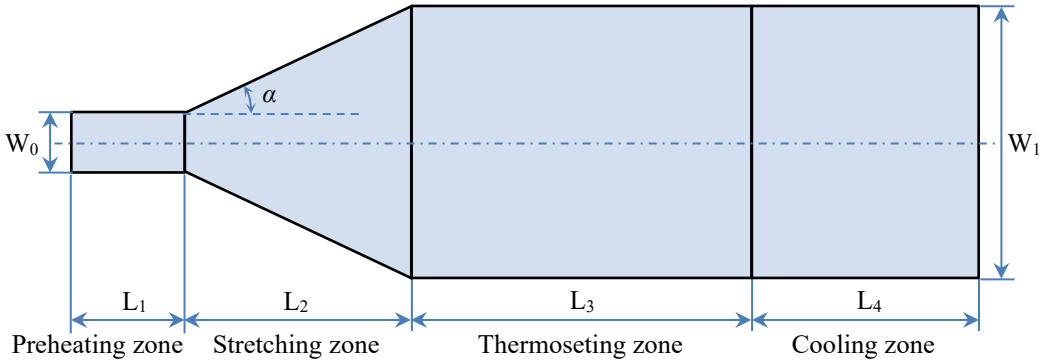

Figure 2: Schematic diagram of a tenter used for transverse stretching of film

Table 1: Lengths of each zone of the pilot plant tenter

Preheating zone	Stretching zone	Heating zone	Cooling zone
L_1	L_2	L_3	L_4
600.0	1200.0	1200.0	1200.0

3 SIMULATION METHOD OF FILM TRANSVERSE STRETCHING

In this study, we proposed a simulation method for the transverse stretching of the successive biaxial stretching in which the kink band phenomenon and the film tearing are observed for the fluorine film. The simulation method is based on the finite element method, and the constitutive equation of the elasto-plastic body considering orthogonal plastic anisotropy is used for the longitudinally stretched fluorine film.

3.1 The target of simulation and finite element model

The target of simulation for this study is the region from inlet of the tenter (preheating zone) to the outlet of the tenter (cooling zone), and the film transversely stretched in the stretching

zone. Figure 3 shows the initial shape in the simulation of the fluorine film after longitudinal stretching. The initial shape is set to a sufficient length with a margin in consideration of the influence of deformation before and after the tenter. Since the fluoropolymer has low rigidity, the protective layers as schematically depicted in Fig.3 (b) are attached to the edges of the film to prevent the film from tearing due to gripping with the tenter clips during transverse stretching. In this study, the protective layer of width W and thickness T is considered in the analysis model.

Considering the symmetry of the tenter shape and the stretching progress situation, the analysis can be performed with a 1/2 symmetry model using the half region above the centerline. Since the film is thin and stretched in-plane, the simulation of the film stretching deformation can be treated as a two-dimensional plane stress problem, and the quadrilateral plane stress element with four nodes is used to mesh the simulation area shown in Fig.3.

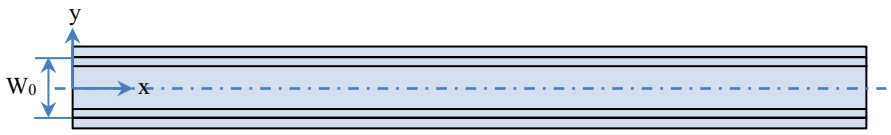

(a) Finite element mesh area

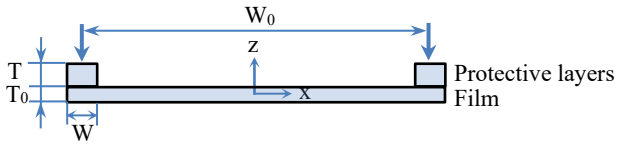

(b) Cross-section of film with protective layers attached on both edges

Figure 3: Longitudinally stretched film region for transverse stretching simulation

3.2 Boundary conditions

The Y-direction displacement of the nodes at the centerline of the film as shown in Fig.3 is constrained to zero due to the symmetry of the tenter shape and the stretching progress situation. In addition, it is assumed that the nodes at both the left and right ends of the film shown in Fig.3 are not constrained and can move freely in the X and Y directions.

3.3 Load conditions

In this study, forced displacement applied to the nodes at the edges of the film, which are griped and moved by the tenter clips, is used as the load conditions to express the transverse stretching in the tenter. Regarding the load conditions of the nodes at the edges of the film gripped by the tenter clips, the following load conditions are applied.

(1) For the nodes before entering the stretching zone, their displacement in the Y direction is constrained to zero and the displacement in the X direction is set to $i \times \delta x$, which is the stretching travel distance in the longitudinal direction, where i is the number of stretching travel steps and δx is the increment of the stretching travel distance for each step.

(2) For the nodes in the stretching zone, their displacement in the Y direction is set to $(i-j+1) \times \delta x \times \sin\alpha$ and the displacement in the X direction is set to $(i-j+1) \times \delta x \times \cos\alpha + (j-1) \times \delta x$, where α is the inclination angle of the stretching zone shown in Fig.2 and j indicates the order of the nodes entering the stretching zone.

(3) For the nodes after exiting the stretching zone, their displacement in the Y direction is set to $(W_1-W_0)/2$ and the displacement in the X direction is set to $i\times\delta x-L_2\times(sec\alpha-1)$.

It should be noted that the load conditions of the nodes at the edges of the film gripped and moved by the tenter clips change from time to time as the film stretching progresses. By using the load conditions, it is possible to express the basic behavior of the film transverse stretching process by the tenter while advancing in the traveling direction. The schematic diagram of the load conditions of the film transverse stretching is shown in Fig.4.

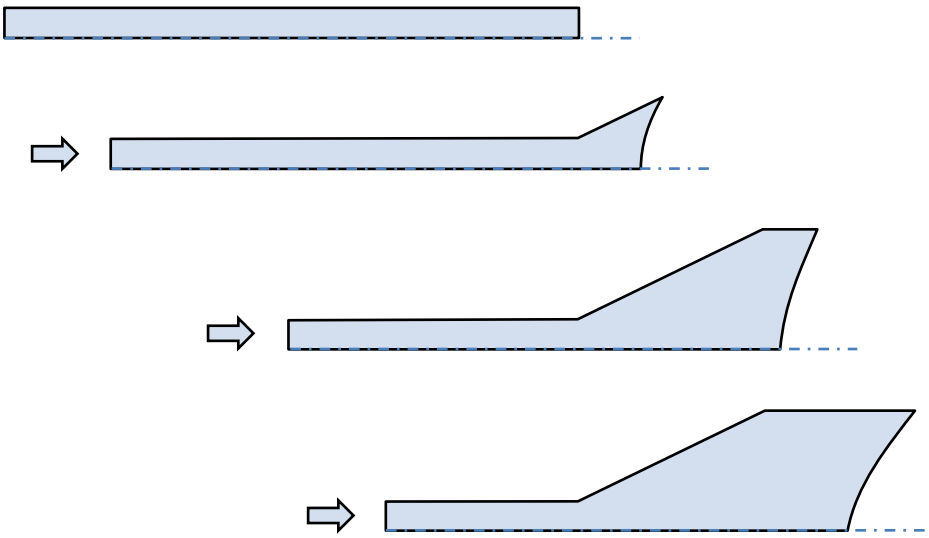

Figure 4: Changes in the forced displacement of the film edge gripped and moved by the tenter clips during transverse stretching, only the film above the center line is shown due to symmetry

3.4 Anisotropic plasticity

The anisotropic potential theory [9] uses Hill's criterion (an extension to the von Mises yield criterion) to account for the anisotropic yield of the material. When this criterion is used with the isotropic hardening option, the yield function is given by:

$$f\{\sigma\} = \sqrt{\{\sigma\}^T[M]\{\sigma\}} - \sigma_0(\bar{\epsilon}^p) \tag{1}$$

where σ is stress and σ_0 is reference yield stress, and $\bar{\epsilon}^p$is equivalent plastic strain, and when it is used with the kinematic hardening option, the yield function takes the form:

$$f\{\sigma\} = \sqrt{(\{\sigma\} - \{\alpha\})^T[M](\{\sigma\} - \{\alpha\})} - \sigma_0 \tag{2}$$

where α is back stress. The material is assumed to have three orthogonal planes of symmetry. Assuming the material coordinate system is perpendicular to these planes of symmetry, the plastic compliance matrix [M] can be written as:

$$[M] = \begin{bmatrix} G+H & -H & -G & 0 & 0 & 0 \\ -H & F+H & -F & 0 & 0 & 0 \\ -G & -F & F+G & 0 & 0 & 0 \\ 0 & 0 & 0 & 2N & 0 & 0 \\ 0 & 0 & 0 & 0 & 2L & 0 \\ 0 & 0 & 0 & 0 & 0 & 2M \end{bmatrix} \tag{3}$$

F, G, H, L, M and N are material constants determined experimentally. They are defined as:

$$F = \frac{1}{2}\left(\frac{1}{R_{yy}^2} + \frac{1}{R_{zz}^2} - \frac{1}{R_{xx}^2}\right),\ G = \frac{1}{2}\left(\frac{1}{R_{zz}^2} + \frac{1}{R_{xx}^2} - \frac{1}{R_{yy}^2}\right),\ H = \frac{1}{2}\left(\frac{1}{R_{xx}^2} + \frac{1}{R_{yy}^2} - \frac{1}{R_{zz}^2}\right)$$
$$L = \frac{3}{2}\left(\frac{1}{R_{yz}^2}\right),\ M = \frac{3}{2}\left(\frac{1}{R_{xz}^2}\right),\ N = \frac{3}{2}\left(\frac{1}{R_{xy}^2}\right) \tag{4}$$

The yield stress ratios R_{xx}, R_{yy}, R_{zz}, R_{xy}, R_{yz} and R_{xz} can be calculated as:

$$R_{xx} = \frac{\sigma_{xx}^y}{\sigma_0},\ R_{yy} = \frac{\sigma_{yy}^y}{\sigma_0},\ R_{zz} = \frac{\sigma_{zz}^y}{\sigma_0},\ R_{xy} = \sqrt{3}\frac{\sigma_{xy}^y}{\sigma_0},\ R_{yz} = \sqrt{3}\frac{\sigma_{yz}^y}{\sigma_0},\ R_{xz} = \sqrt{3}\frac{\sigma_{xz}^y}{\sigma_0} \tag{5}$$

where σ_{xx}^y is yield stress values, The plastic slope is calculated as:

$$E^{pl} = \frac{E_x E_t}{E_x - E_t} \tag{6}$$

where E_x is elastic modulus in x-direction, and E_t is tangent modulus defined by the work hardening coefficient.

3.5 Material properties

In the longitudinal-transverse successive biaxial stretching, the film entering the tenter is already longitudinally stretched, so its material properties are significantly different from those of the unstretched film. Therefore, in this study, tensile test is carried out on the longitudinally stretched film. The test piece is cut out from the center of the film in the width direction by 15mm (width) × 150mm (length). The test is performed 3 times, and the average value thereof is used. In a large deformation problem such as transverse stretching analysis, true stress-strain curve converted from nominal stress-strain curve obtained by a tensile test is used. The true stress-strain curves of the fluorine films, which are stretched at the longitudinal stretching ratios of 1.8, 2.0, 2.2 and 2.4, respectively, in the transverse direction obtained in the tensile tests at 60℃ are shown in Fig.5, where MD18x etc. in the figure represent the longitudinal stretching ratios. The true stress-strain curve of the cast polypropylene (CPP) of the protective layer is also shown in Fig.5. The elastic moduluses, yield stresses and work hardening coefficients used in the simulation are calculated from true stress-strain curves, and the Poisson's ratio is 0.46.

In film stretching, elastic deformation is generally very small and plastic deformation is dominant. Therefore, when analyzing deformation behavior of a film in the stretching process,

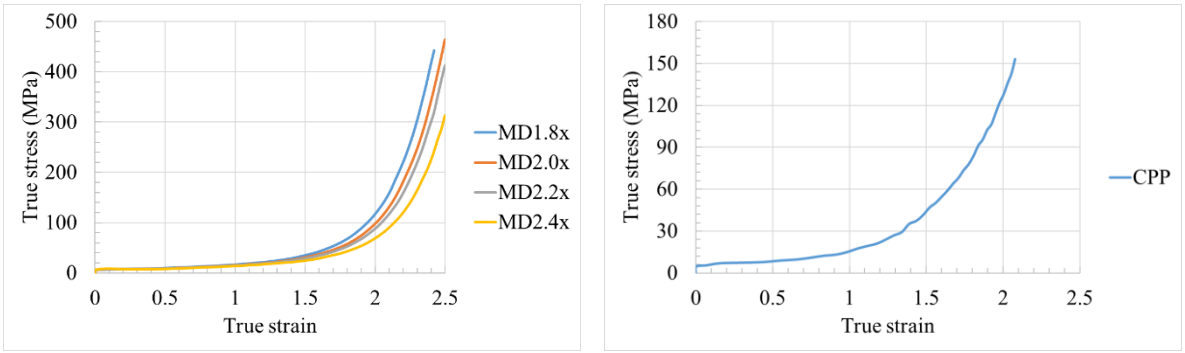

Figure 5: True stress-strain curves of the fluorine film and protective layer of CPP

it is considered that the deformation of the film basically follows the elasto-plastic law or the rigid-plastic law. In elasto-plastic theory, it is necessary that the elastic modulus must be larger than the work hardening coefficients. However, in the orientation hardening region of the fluorine film, the work hardening coefficients are found to be larger than the elastic modulus. In such a case, the elastic modulus is set to 1.1 times the maximum work hardening coefficient so that the elasto-plastic theory can be applied to the simulation. It is estimated that this setting has little effect on the results because the elastic deformation is very small in the film stretching.

4 EXPERIMENT

The experiments are performed with fluoropolymer using the pilot plant as schematically shown in Fig 1. The details of the longitudinal stretching and the transverse stretching of the fluorine film performed at 60℃ are described below. In this study, the stretched film thickness is expressed as a value normalized by using the unstretched film thickness of 0.04mm.

4.1 Longitudinal stretching

In this study, the fluorine film is stretched in the longitudinal direction at stretching ratios of 1.8, 2.0, 2.2 and 2.4, respectively. Each test is performed 3 times. The thickness distribution in the width direction of the longitudinally stretched fluorine film at different stretching ratios is shown in Fig.6. Here, the horizontal axis uses the normalized film width, 0 and 1 correspond to both edges of the fluorine film, and the longitudinal stretching ratios are expressed as MD1.8x, MD2.0x, MD2.2x and MD2.4x, respectively. It can be read that the occurrence of thickness unevenness after longitudinal stretching is observed.

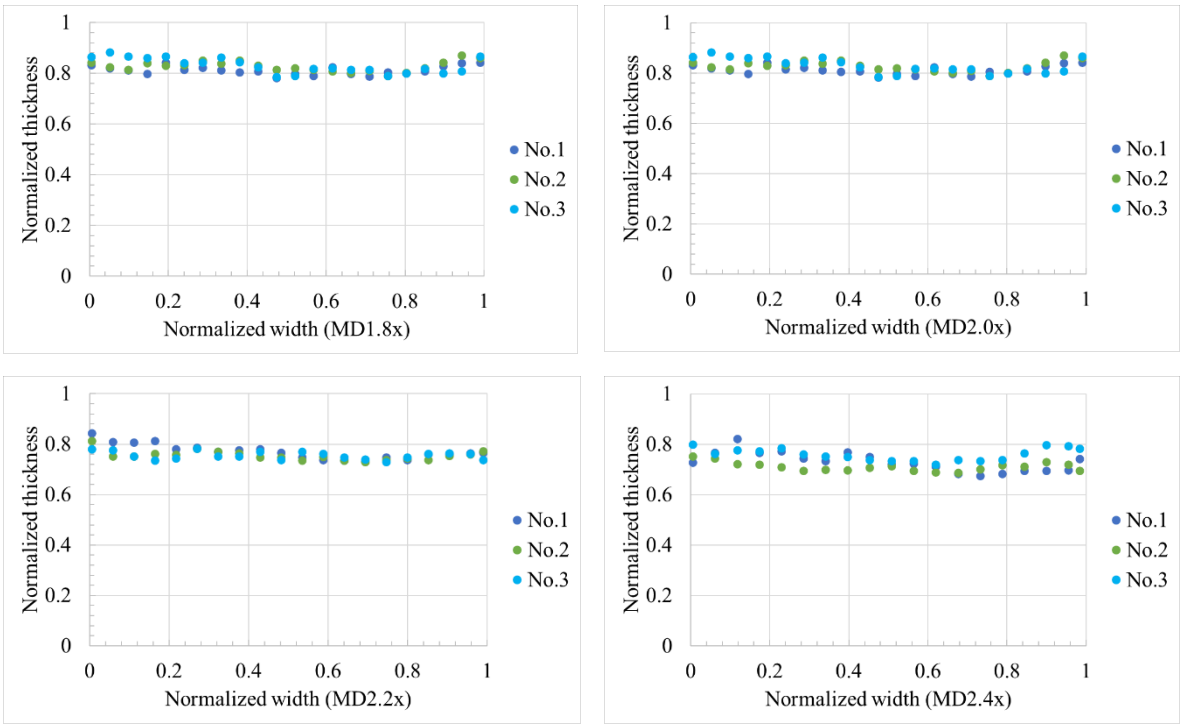

Figure 6: Normalized thickness distribution in width of longitudinally stretched film at different stretching ratios

Table 2: Specifications of the fluorine film after different longitudinal stretching ratios

Item name	Size (mm)	Longitudinal stretching ratios			
		1.8	2.0	2.2	2.4
Fluorine film	Thickness, $T_0 \times 10^{-3}$	32.9	31.8	30.4	29.4
	Width W_0	180.0	168.0	155.0	145.0
	Width W_1	810.0	756.0	698.0	653.0
Protective layer	Thickness, $T \times 10^{-3}$	57.0	54.0	55.0	50.0
	Width, W	35.0	33.5	32.0	29.5

4.2 Transverse Stretching

In this study, the different longitudinally stretched fluorine film is transversely stretched at a stretching ratio of 4.5 with the pilot plant tenter. Since the longitudinal stretching ratios are different, the thickness and the width of the fluorine film entering the transverse stretching after the longitudinal stretching are also different. Table 2 shows the average thickness and width of the longitudinally stretched fluorine films and the protective layers at the longitudinal stretching ratios of 1.8, 2.0, 2.2 and 2.4, respectively, for the transverse stretching. The test results of the transverse stretching of the fluorine film will be described together with the simulation results in the next section.

5 SIMULATION RESULTS AND TEST RESULTS

Using the above-mentioned simulation model and boundary conditions and load conditions, the deformation behavior of the longitudinally stretched fluorine film during the transverse stretching is analyzed. The finite element method software ANSYS [10] is used for the analysis.

In this study, it is assumed that the longitudinally stretched fluorine film is an elasto-plastic body having orthogonal anisotropy, and its material properties follow the formulas shown in Section 3.4. Generally, the yield stress ratios R_{ij} shown in Eq. (5) should be obtained by the material tests, but it is difficult to carry out these material tests in practice. Therefore, in this study, it is assumed that the longitudinally stretched fluorine film is isotropic in the cross section perpendicular to the longitudinal direction, and the ratios R_{xx}, R_{yy}, R_{zz}, R_{xy}, R_{yz} and R_{xz} is set to be 1, R, R, R, R, R, where R is referred to as a plastic anisotropy index, and when its value is 1, it corresponds to an isotropic body. In the analysis, the average thickness shown in Table 2, which is calculated based on the thickness distribution in the width direction displayed in Fig.6, is used as the initial thickness for transverse stretching simulation of the fluorine film. The deformation behavior of the fluorine film during transverse stretching is investigated when the value of R is changed.

Figure 7 shows the calculation results and the test results of the normalized thickness distribution in the width of the fluorine film stretched at the longitudinal stretching ratios of 1.8, 2.0, 2.2 and 2.4, respectively, and the transverse stretching ratio of 4.5. The horizontal axis is a normalized width of the film, 0 and 1 represent both edges, and 0.5 represents the center. Here, the calculation results take the values at the position of the outlet of the thermosetting zone.

For the fluorine film stretched with longitudinal and transverse stretching ratios of 1.8 and 4.5 (also expressed as MD1.8x×TD4.5x), respectively, the stretching simulation is performed with the plastic anisotropy index R set to 0.79. It is found that the calculation results and the test results are almost the same for the fluorine film thickness. It is also clarified that the

simulation considering the plastic anisotropy index R can reproduce the occurrence of the kink band phenomenon observed in the experiment during the transverse stretching of the fluorine film. The kink band is a phenomenon in which a portion where the film is hardly stretched occurs in the transverse stretching process. However, the calculation results and the test results are different for the position where the kink band phenomenon occurs. This is probably because the initial thickness of the film is set to a uniform value and a symmetric model is used in the simulation. In fact, as shown in Fig.6, the initial thickness of the fluorine film is not uniform, and the temperature distribution in the tenter is not uniform [11]. As a result, it seems that the position where the kink band phenomenon occurs in the transverse stretching process of the fluorine film is not symmetrical. Furthermore, it is clarified that by attaching the protective layers to both edges of the fluorine film, the film is less likely to be stretched near the edges, and this has the effect of preventing the film from tearing due to gripping of the tenter clips.

For the fluorine film stretched with longitudinal and transverse stretching ratios of 2.0 and 4.5 (MD2.0x×TD4.5x), respectively, the stretching simulation is performed with the plastic anisotropy index R set to 0.83. As in the case of MD1.8x×TD4.5x above, the calculation results and the test results are almost the same for the thickness, but the position where the kink band phenomenon occurs is different.

For the fluorine film stretched with longitudinal and transverse stretching ratios of 2.2 and 4.5 (MD2.2x×TD4.5x), respectively, the stretching simulation is performed with the plastic anisotropy index R set to 0.86. It is found that the calculation results and the test results are in good agreement. In addition, unlike the case of MD1.8x×TD4.5x and MD2.0x×TD4.5x above, no kink band phenomenon is observed in the transverse stretching of the fluorine film.

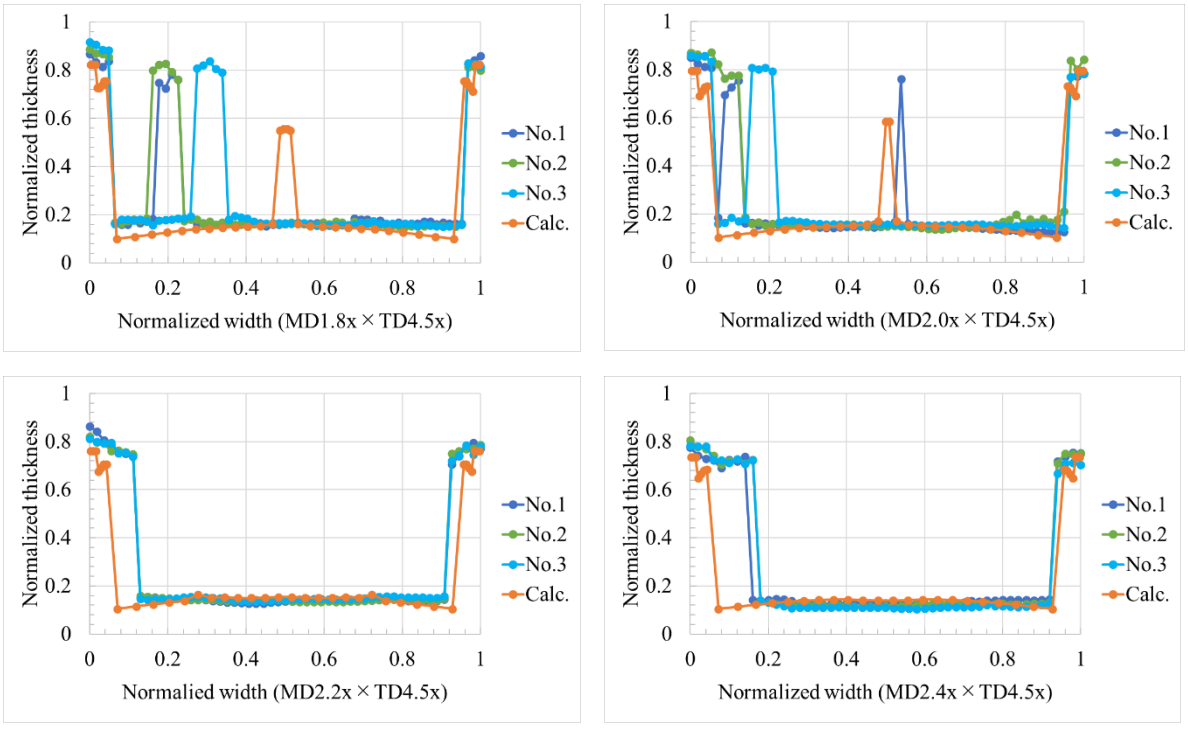

Figure 7: Normalized thickness distribution in width of fluorine film with longitudinal and transverse stretching ratios of MD1.8x×TD4.5x, MD2.0x×TD4.5x, MD2.2x×TD4.5x and MD2.4x×TD4.5x, respectively

For the fluorine film stretched with longitudinal and transverse stretching ratios of 2.4 and 4.5 (MD2.0x×TD4.5x), respectively, the stretching simulation is performed with the plastic anisotropy index R set to 0.90. As in the case of MD2.2x×TD4.5x above, in the transverse stretching of the fluorine film, the calculation results and the test results for the thickness are almost the same, and the occurrence of the kink band phenomenon is not observed.

Figure 8 illustrates the normalized thickness distribution of the fluorine film during the transverse stretching process. It can be seen from the figure that the kink band phenomenon occurs near the center of the fluorine film in the case of MD1.8x×TD4.5x and MD2.0x×TD4.5x and does not occur in the case of MD2.2x×TD4.5x and MD2.4x×TD4.5x.

Summarizing the above, it become clear that the behavior of film deformation during the transverse stretching process can be calculated by appropriately setting the plastic anisotropy index R. However, since it is difficult to obtain the plastic anisotropy index R by the material tests, a realistic approach is to identify R by comparing the calculation results and test results in the transverse stretching. The identified R can be associated with birefringence of the film to obtain a regression equation, which can be used to predict the value of R.

Figure 9 shows the relationship between the plastic anisotropy index R and the birefringence, and the longitudinal stretching ratio of the longitudinally stretched fluorine film. In this study, the difference in the main axis refractive index of the longitudinally stretched fluorine film, that is, the birefringence is used as an index of the molecular orientation. The birefringence is measured at three points in the longitudinal stretched fluorine film, and the average value is used. It is found that the plastic anisotropy index of the longitudinally stretched fluorine film has an almost linear relationship with the birefringence and the longitudinal stretching ratio.

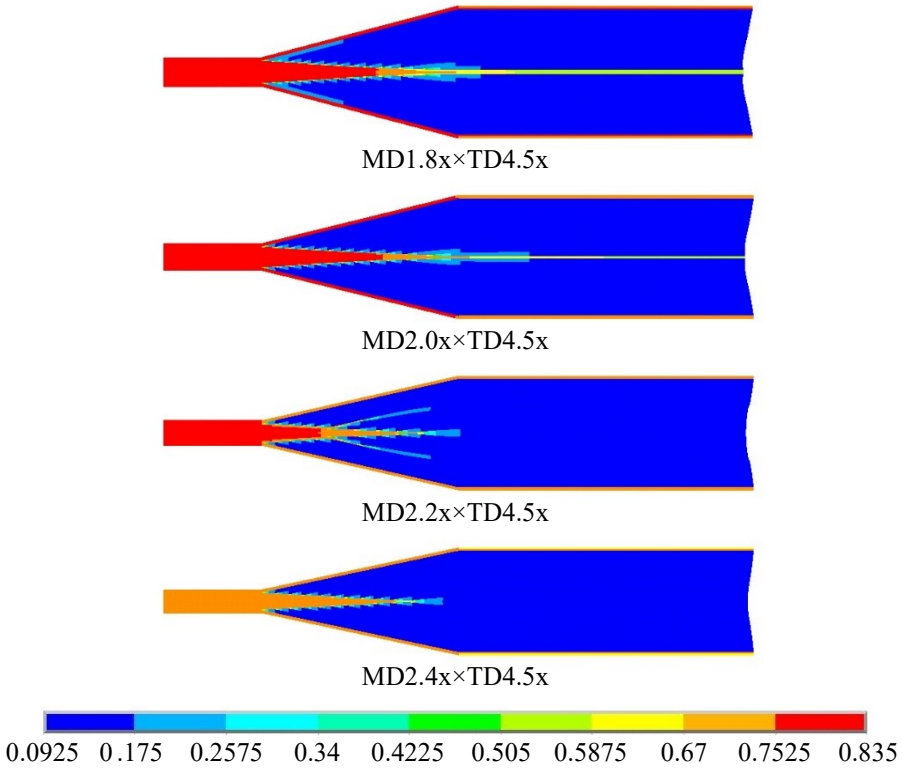

Figure 8: Normalized thickness distribution of fluorine film in transverse stretching process

Figure 10 shows the change in the normalized thickness distribution of the fluorine film due to the difference in the length L_2 of the stretching zone. Here, L_2 is represented by the dimensionless parameter r defined by $r = L_2/(W_0 - W_0)$.

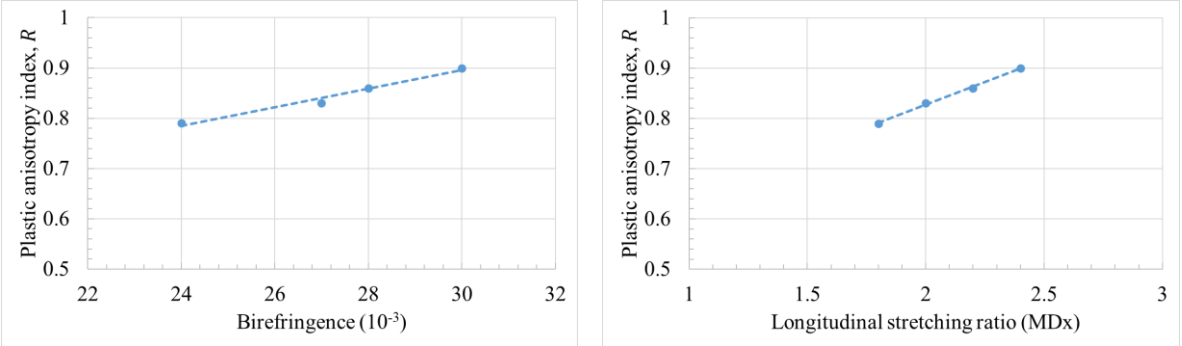

Figure 9: Relationship between the plastic anisotropic index and the birefringence, and the longitudinal stretching ratio of the longitudinally stretched fluorine film

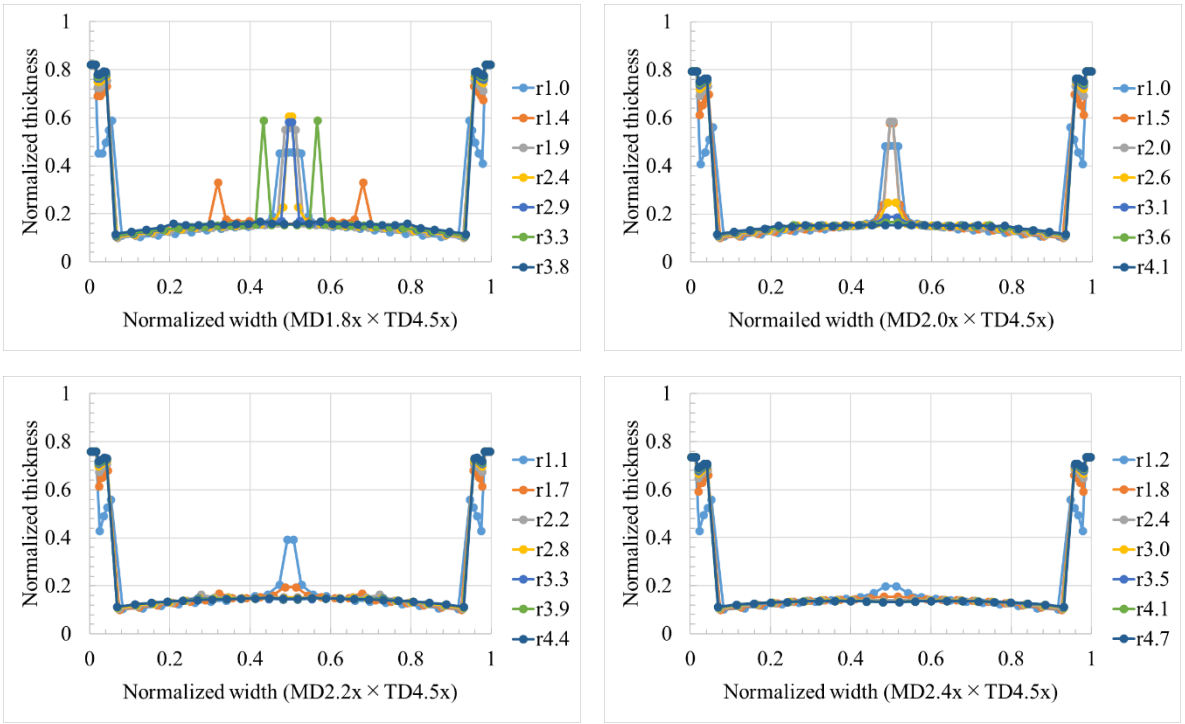

Figure 10: Normalized thickness distribution in width of fluorine film with different stretching zone length

In the case of stretching ratios of MD1.8x×TD4.5x and MD2.0x×TD4.5x, it is found that the kink band phenomenon does not occur if the stretching zone length is extended from the current $r1.9$ to $r3.8$ or more, and from the current $r2.0$ to $r3.3$ or more, respectively. On the other hand, in the case of the stretching ratios of MD2.2x×TD4.5x and MD2.4x×TD4.5x, it is found that the kink band phenomenon occurs when the stretching zone length is shortened from the current $r2.2$ to $r1.7$ or less, and from the current $r2.4$ to $r1.2$ or less.

6 CONCLUSIONS

In this study, we proposed a simulation method for film transverse stretching based on the finite element method using the orthogonal anisotropy plastic model. The simulation method can reproduce the occurrence of the kink band phenomenon during the transverse stretching by a tenter. Moreover, since the calculation results and the test results are almost the same, it can be said that the simulation method is appropriate. The main conclusions are as follows.

- The presence or absence of the kink band phenomenon during the transverse stretching largely depends on the plastic anisotropy index of the longitudinally stretched film.
- The plastic anisotropy index of the longitudinally stretched fluorine film has an almost linear relationship with the birefringence and the longitudinal stretching ratio.
- Increasing the length of the stretching zone has the effect of reducing the occurrence of the kink band phenomenon during the transverse stretching.
- The protective layers attached to the edges of the film have the effect of preventing the film from tearing due to gripping of the tenter clips during the transverse stretching.

REFERENCES

[1] Ebnesajjad, S. *Introduction to Fluoropolymers: Materials, Technology, and Applications (Second Edition)*. William Andrew, (2020).

[2] Hazama, T., Komatsu, N., Yokotani, K., Tatemichi, M. and Higuchi, T. and Koga, K. Film. Pub. No. US 2020/0032014 A1 (2020).

[3] Yamada, T. and Nonomura, C. An attempt to simulate the bowing phenomenon in tenter with simple models. *J. Appl. Polym. Sci.* (1993) **48**:1399-1408.

[4] Yamada, T., Nonomura, C. and Matsuo T. Attempt to reduce bowing distortion in tentering of film. *J. Appl. Polym. Sci.* (1994) **52**:1393-1403.

[5] Yamada, T., Nonomura, C. and Matsuo, T. Analyses of bowing phenomena in successive transverse stretching and thermosetting process for biaxially oriented film. *Int. Polym. Process. X* (1995) **4**:334-340.

[6] Sugihara, G., Iwasaki, T., Yamada, T., Yokoyama, A. and Fukunaga, M. Influence of process conditions on bowing phenomenon in successive biaxial stretching with tenter. *Materials Processing and Design: Modeling, Simulation and Applications*, *NUMIFORM 2004*, edited by S. Ghosh, J. C. Castro, and J. K. Lee. *American Institute of Physics* (2004): 1453-1458.

[7] Tokihisa, M., Kushizaki, Y., Tomiyama, H. and Yamada, T. The deformation behavior of polypropylene film during transverse direction stretching under different draw ratio along machine direction. *Asian Workshop on Polymer Processing, Book of Extended Abstracts* (2012):159-162.

[8] https://www.jsw.co.jp/en/product/plastics_machinery/film.html (accessed on 9 May 2022).

[9] Hill, R. *The Mathematical Theory of Plasticity*. Oxford University Press. New York (1983).

[10] ANSYS Mechanical APDL 19.0 (2018).

[11] Tokihisa, M., Kushizaki, Y., Tomiyama, H., Yamamoto, Y. and Yamada, T. Prediction of film stretching behavior in tenter for transverse stretching in consideration of heated air flow, *Asian Workshop on Polymer Processing, Book of Extended Abstracts* (2008):31-32.